Cardiovascular Engineering and Technology, Vol. 10, No. 1, March 2019 *(© 2018)* pp. 155–172
https://doi.org/10.1007/s13239-018-00379-x

Effect of Varying Viscosity on Two-Fluid Model of Blood Flow through Constricted Blood Vessels: A Comparative Study

ASHISH TIWARI and SATYENDRA SINGH CHAUHAN

Department of Mathematics, Birla Institute of Technology and Science Pilani, Pilani, Rajasthan 333 031, India

(Received 4 April 2018; accepted 18 September 2018; published online 9 October 2018)

Associate Editors Ajit P. Yoganathan and David Elad oversaw the review of this article.

Abstract

Purpose—Most of the previously studied non-Newtonian blood flow models considered blood viscosity to be constant but for correct measurement of flow rate and flow resistance, the hematocrit dependent viscosity will be better as various literature suggested the variable nature of blood viscosity. Present work concerns the steady and pulsatile nature of blood flow through constricted blood vessels. Two-fluid model for blood is considered with the suspension of all the RBCs (erythrocytes) in the core region as a non-Newtonian (Herschel–Bulkley) fluid and the plasma in the cell free region near wall as a Newtonian fluid. No slip condition on the wall and radially varying viscosity has been taken. *Methods*—For steady flow the analytical approach has been taken to obtain the exact solution. Regular perturbation expansion method has been used to solve the governing equations for pulsatile flow up to first order of approximation by assuming the pulsatile Reynolds number to be very small (much less than unity). *Results*—Flow rate, wall shear stress and velocity profile have been graphically analyzed and compared with constant viscosity model. A noteworthy observation of the present study is that rise in viscosity index leads to decay in velocity, velocity of plug flow region, flow rate while flow resistance increases with rising viscosity index (m). The results for Power-law fluid (PL), Bingham-plastic fluid (BP), Newtonian fluid (NF) are found as special cases from this model. Like the constant viscosity model, it has been also observed that the velocity, flow rate and plug core velocity of two-fluid model are higher than the single-fluid model for variable viscosity.

Conclusions—The two-phase fluid model is more significant than the single-fluid model. Effect of viscosity parameter on various hemodynamical quantities has been obtained. It is also concluded that a rising viscosity parameter (varying nature of viscosity) significantly distinguishes the single and two-fluid models in terms of changes in blood flow resistance. The outcome of present study may leave a significant impact on analyzing blood flow through small blood vessels with constriction, where correct measurement of flow rate and flow resistance for medical treatment is very important.

Keywords—Two-fluid model, Steady and pulsatile flow, Herschel–Bulkley fluid, Time-dependent constriction, Variable viscosity.

NOMENCLATURE

$'\_'$	The dimensional quantities
r	Distance in radial direction
z	Distance in axial direction
t	Time
R_p	Plug core (flow) radius
R_{p0}, R_{p1}	Zeroth and first order approximation of plug core (flow) radius, respectively
u_H, u_N	Axial velocities in core and plasma region, respectively
u_{H0}, u_{N0}	Zeroth order approximation of axial velocity in core and plasma region, respectively
u_{H1}, u_{N1}	First order approximation of axial velocities in core and plasma region, respectively
u_p	Plug core velocity
u_{p0}, u_{p1}	Zeroth and first order approximation of plug core velocity, respectively
n	Herschel–Bulkley fluid parameter
m	Viscosity index
K	Constant in viscosity relation
p	Pressure
$p_s, q(z)$	Steady state pressure gradients for steady and pulsatile flow, respectively
$Q_s, Q(z,t)$	Volumetric flow rate for steady and pulsatile flow, respectively
$R_1(t,z)$	Radius of artery with time-dependent stenosis in core region
$R(t,z)$	Radius of artery with time-dependent

Address correspondence to Ashish Tiwari, Department of Mathematics, Birla Institute of Technology and Science Pilani, Pilani, Rajasthan 333 031, India. Electronic mail: ast79.ashish@gmail.com, sdg25792@gmail.com

	stenosis in plama region
$R_1(z)$	Radius of artery with stenosis in steady state case (core region)
$R(z)$	Radius of artery with stenosis in steady state case (plama region)
R_0	Radius of normal artery
A	Amplitude
L	Length of the constricted blood vessel

Greeks letters

τ_H, τ_N	Shear stresses in core and plasma region, respectively
τ_{H0}, τ_{N0}	Zeroth order approximation of shear stress in core and plasma region, respectively
τ_{H1}, τ_{N1}	First order approximation of shear stress in core and plasma region, respectively
τ_y	Yield stress
θ	Dimensionless yield stress
τ_w	Wall shear stress
ρ_H, ρ_N	Densities of blood in core and plasma region, respectively
μ_H, μ_N	Constant viscosities of the blood in core and plasma region, respectively
$\mu'_H(r)$	Variable viscosity of the blood in core region
ρ_0	The ratio of densities in plasma and core region
α	Womersley frequency parameter
δ_H, δ_N	Peak height of stenosis in core and plasma region, respectively
ω	Angular frequency
λ_s, λ	Flow resistance for steady and pulsatile flow, respectively

Subscripts

0	Zeroth order approximation (for $R_{p0}, u_{H0}, u_{p0}, \tau_{H0}, \tau_{N0}$)
1	First order approximation (for $R_{p1}, u_{H1}, u_{p1}, \tau_{H1}, \tau_{N1}$)
H	Herschel–Bulkley fluid (for $u_H, \tau_H, \delta_H, \rho_H$)
N	Newtonian fluid (for $u_N, \tau_N, \delta_N, \rho_N$)
p	Plug flow value(for u_p, R_p)
s	Steady flow value (for p_s, Q_s, λ_s)
w	Value at wall (for τ_w)
y	Value at yield stress (for τ_y)

INTRODUCTION

The study of physical mechanism of blood flow through blood vessels in the cardiovascular system is fundamental understanding of cardiovascular diseases, like atherosclerosis and post-stenotic dilation. Blood circulation through blood vessels is a complex phenomenon, so researchers or mathematicians found it difficult to formulate the mathematical problems in the form of simple or relevant models which are mathematically simple and physically significant. Hence, the mathematical modeling and analysis of these procedures can contribute to enhance the pathological and clinical planning. Despite several complications, the mathematicians kept working on the mathematical formulations for the suitable constitutive models to analyze blood flow through blood vessels. Womersley[41] made a significant progress in this direction when he found an analytic expression to describe the flow of blood through a rigid tube and described methods to compute velocity, shear stress and vascular impedance. Acknowledging the non-Newtonian behaviour of blood in smaller blood vessels, MacDonald,[13] Dash *et al.*[10] and Sankar and Hemalatha[29] studied the non-Newtonian fluid flow through stenotic/catheterized blood vessels by considering the flow to be steady and observed the effect of the catheter radius and yield stress on hemodynamical quantities such as velocity profile, yield plane location (which can be obtained by knowing plug flow radius), flow rate, wall shear stress and flow resistance. They found that wall shear stress and flow resistance increases with yield stress whereas flow resistance and wall shear stress decreases with increase of catheter radius. Among above works, the Herschel–Bulkley fluid model is very useful in modeling blood flow through small vessels as it works well for both the moderate as well as high shear rate.[29] Casson fluid is used by many researchers to model the blood flow through small blood vessels at low shear rate as the results obtained under these circumstances matches with Herschel–Bulkley fluid model at low shear rate. Aroesty and Gross[2,3] mathematically examined the pulsatile nature of Casson fluid flow through small blood vessels which possess the finite yield stress and shear-dependent viscosity.

The most common cardiovascular disease is atherosclerosis which occurs due to the deposition of fatty plaques of cholesterol on different parts of arterial wall in which the flow resistance increases due to narrowing of the area of the flow region. Many investigators Young,[43] Shukla *et al.*,[37] Chaturani and Samy[8,9] have theoretically studied the blood flow through constricted blood vessel and observed that the effect of shear-dependent viscosity and yield stress on hemodynamical quantities such as wall shear stress, flow rate and flow resistance *etc*. Sankar and Hemalatha[28] and Sankar and Lee[32] analyzed the combined effect of pulsatility, stenosis size and non-Newtonian behavior of blood through constricted blood vessels by assuming blood as non-Newtonian Herschel–Bulkley fluid and found that the values of plug flow radius of Herschel–Bulkley fluid are slightly higher than the Casson fluid. It

is also noticed that flow resistance increases with the increase in height of stenosis and yield stress while all other parameters are kept fixed. The effect of non-Newtonian nature of blood and pulsatility on flow through constricted blood vessels is observed by Siddiqui *et al.*[38] by assuming the blood as non-Newtonian Casson fluid. Nagarani and Sarojamma[21] examined the effect of external body acceleration on pulsatile flow of Casson fluid through blood vessel with mild constriction and observed that periodic body acceleration leads to enhanced flow rate and reduced flow resistance. Mekheimer and Kot[15] mathematically analyzed two-dimensional blood flow through concentric tubes where inner tube represented the catheter and outer tube represented the constricted blood vessel. Recently, Thanaa *et al.*[11] discussed the Cu-model for blood flow through catheterized constricted blood vessels with a thrombosis and concluded that velocity distribution increases with increase in nanofluid volume fraction whereas flow impedance decreases.

In all the above work, blood viscosity was assumed to be constant but physically the blood viscosity depends on hematocrit (the volume concentration of all red blood cells in whole blood) and diameter of the blood vessel proposed by Lih.[12] This assumption is physically more realistic in modeling blood flow through blood vessels. Keeping this fact in mind, Misra and Ghosh[20] carried out the analysis for steady and pulsatile nature of blood flow through blood vessels with parent artery in which the blood is considered as Casson fluid and examined the effect of variation of hematocrit on fluid flow quantities. The combined effect of external magnetic field and radially varying viscosity on blood flow through blood vessels with constriction was examined by Bali and Awasthi[4] in which they solved the non-linear pressure equation with series method. A theoretical study of blood flow through tapered overlapping constricted blood vessels with varying nature of viscosity depending on hematocrit was presented by Shit *et al.*[35] in which the governing equations for incompressible, Newtonian fluid with suitable boundary conditions were solved by the well known Frobenius series method. Mekheimer and Abd Elmaboud[14] discussed the simultaneous effect of varying viscosity and thermal conductivity on pulsatile flow through a vertical asymmetric channel.

All the above studies involve the position dependent constriction for blood flow through blood vessel. However, under different circumstances growth into the arterial wall of uniform cross-section may be time-dependent[42] which plays a significant role in the diagnosis and clinical treatment[6,19] of various cardiovascular diseases. Sankar and Lee[34] numerically investigated MHD flow of a non-Newtonian fluid through blood vessels with time-dependent constriction. Mekheimer and Kot[16] mathematically analyzed the unsteady flow of Sisko fluid through tapered elastic blood vessel with time-dependent overlapping constriction. A theoretical investigation of pulsatile flow through a time-dependent constricted blood vessel under periodic body acceleration was carried out by Sinha *et al.*[39] Recently, the effect of catheterization on blood flow through curved blood vessel with time-variant overlapping constriction has been studied by Mekheimer and Kot[17] by using the rectangular toroidal coordinate system. Mekheimer *et al.*[18] discussed the unsteady flow of a Carreau fluid through inclined catheterized blood vessels having clot model with time-dependent overlapping constriction.

Apart from the nature of single-fluid model of blood flow though arteries, it is also important to see when the blood flows through small blood vessels, blood behaves as non-Newtonian fluid in the core region (representing RBCs) and Newtonian fluid in the cell free region near wall that plays a significant role in the flow convention of the system. Bugliarello and Sevilla[5] experimentally verified the existence of a cell free region near the wall representing plasma. Several researchers have worked on two-fluid model of blood flow through stenosed arteries with blood being non-Newtonian fluid in core region and Newtonian fluid in cell free region. Chaurani and Kaloni,[7] Shukla *et al.*,[36] Srivastava and Saxena,[40] Sankar and Usik Lee,[31,33] Sankar and Ismail[30] have analyzed the blood flow through stenotic arteries by treating the blood as two-fluid model. They investigated the effect of peripheral layer viscosity and size of stenosis on the physiological characteristic of blood flow through constricted blood vessels. Ponalagusamy and Tamil Selvi[23] considered the two-layered model of blood flow through constricted blood vessels with varying peripheral layer thickness near wall and obtained the analytical expressions for the same. Recently, Ponalagusamy and Tamil Selvi[24] considered two-layer model of blood flow through a constricted blood vessel in the presence of transverse magnetic field and radially varying viscosity and assumed blood as Newtonian fluid in both the regions. The numerical solutions for hemodynamical quantities such as velocity distribution, flow rate, flow resistance were obtained and the effect of various parameters on these quantities were studied. To the best of our knowledge and on the basis of above literature survey, it is observed that the varying nature of viscosity on two-fluid models has not been given much attention while modeling non-Newtonian fluid flow through blood vessels with constriction by assuming the blood in the core region as Herschel–Bulkley fluid.

In the present analysis, we are going to analyze the effect of varying nature of viscosity instead of constant viscosity model to the blood flow through blood vessel

with constriction. The two-fluid model for blood flow is considered with suspension of all the RBCs (erythrocytes) in the core region as non-Newtonian (Herschel–Bulkley) fluid and the cell free region of plasma as Newtonian fluid. Analytical expressions for the velocity profile, plug core velocity, flow rate and resistance to flow have been obtained. The effect of variable viscosity on hemodynamical quantities such as velocity profile, velocity in plug core region, flow rate and flow resistance are analyzed graphically and compared with the constant viscosity model.

MATHEMATICAL FORMULATION

Consider two-dimensional axially symmetric, laminar, pulsatile and fully developed flow of blood through a constricted blood vessel as shown in Fig. 1. Cylindrical polar coordinates $(\bar{r}, \bar{\phi}, \bar{z})$ have been used with $\bar{r}$, $\bar{z}$ being the radial and axial coordinates, respectively and $\bar{\phi}$ is the azimuthal angle whose origin is located on the vessel axis and the velocity components are $(w, 0, u)$. Two-fluid model for blood flow has been employed. The walls of the constricted blood vessel are assumed to be rigid. For arteries with mild stenosis $(\bar{\delta}_N/\bar{R}_0 \ll 1$, Fig. 1), the radial component of momentum equations will be reduced to $\frac{\partial \bar{p}}{\partial \bar{r}} = 0$.[1,25,27,42]

In this case, the governing equations are

$$\bar{\rho}_H \frac{\partial \bar{u}_H}{\partial \bar{t}} = -\frac{\partial \bar{p}}{\partial \bar{z}} - \frac{1}{\bar{r}} \frac{\partial}{\partial \bar{r}} (\bar{r}\bar{\tau}_H), \quad 0 \le \bar{r} \le \bar{R}_1(\bar{t}, \bar{z}), \quad \text{(1a)}$$

$$\bar{\rho}_N \frac{\partial \bar{u}_N}{\partial \bar{t}} = -\frac{\partial \bar{p}}{\partial \bar{z}} - \frac{1}{\bar{r}} \frac{\partial}{\partial \bar{r}} (\bar{r}\bar{\tau}_N), \quad \bar{R}_1(\bar{t}, \bar{z}) \le \bar{r} \le \bar{R}(\bar{t}, \bar{z}), \quad \text{(1b)}$$

where the shear stress $\bar{\tau} = |\bar{\tau}_{\bar{r}\bar{z}}| = -\bar{\tau}_{\bar{r}\bar{z}}$ (since $\bar{\tau} = \bar{\tau}_H$ or $\bar{\tau} = \bar{\tau}_N$); $\bar{\rho}_H$ and $\bar{\rho}_N$ are densities of blood in core and plasma region, respectively; $\bar{p}$ pressure; $\bar{u}_H$, $\bar{u}_N$ axial velocities in core and plasma region, respectively; $\bar{t}$ time and $\bar{\tau}_H, \bar{\tau}_N$ the shear stresses in core and plasma region, respectively.

For the Herschel–Bulkley fluid (blood) $\bar{\tau}_H$ and Newtonian fluid $\bar{\tau}_N$ are given by

$$\bar{\tau}_H = \bar{\tau}_y + \left[\bar{\mu}'_H(\bar{r})\left(-\frac{\partial \bar{u}_H}{\partial \bar{r}}\right)\right]^{\frac{1}{n}}, \quad \text{if } \bar{\tau} \ge \bar{\tau}_y,\ \bar{R}_p \le \bar{r} \le \bar{R}_1(\bar{t}, \bar{z}), \quad \text{(2a)}$$

$$\frac{\partial \bar{u}_H}{\partial \bar{r}} = 0, \quad \text{if } \bar{\tau} \le \bar{\tau}_y, \quad 0 \le \bar{r} \le \bar{R}_p, \quad \text{(2b)}$$

$$\bar{\tau}_N = \bar{\mu}_N\left(-\frac{\partial \bar{u}_N}{\partial \bar{r}}\right), \quad \bar{R}_1(\bar{t}, \bar{z}) \le \bar{r} \le \bar{R}(\bar{t}, \bar{z}), \quad \text{(2c)}$$

where $\bar{\mu}'_H(\bar{r})$ denote the radially varying viscosity in core region which is $\bar{\mu}'_H(\bar{r}) = \bar{\mu}_H \left\{1 + K - K\left(\frac{\bar{r}}{\bar{R}_0}\right)^m\right\}$[20,24]; $\bar{\mu}_H$ and $\bar{\mu}_N$ constant viscosity coefficient in core and plasma region, respectively; $\bar{\tau}_y$ the yield stress; n Herschel–Bulkley fluid parameter; m is the viscosity index appearing in the expression for variable viscosity and K is constant in viscosity relation.

The boundary conditions are given as

$$\begin{aligned} &\bar{\tau}_H \text{ is finite at } \bar{r} = 0, \\ &\bar{\tau}_H = \bar{\tau}_N,\ \bar{u}_H = \bar{u}_N \text{ at } r = \bar{R}_1(\bar{t}, \bar{z}), \\ &\bar{u}_N = 0 \text{ at } \bar{r} = \bar{R}(\bar{t}, \bar{z}). \end{aligned} \quad \text{(3)}$$

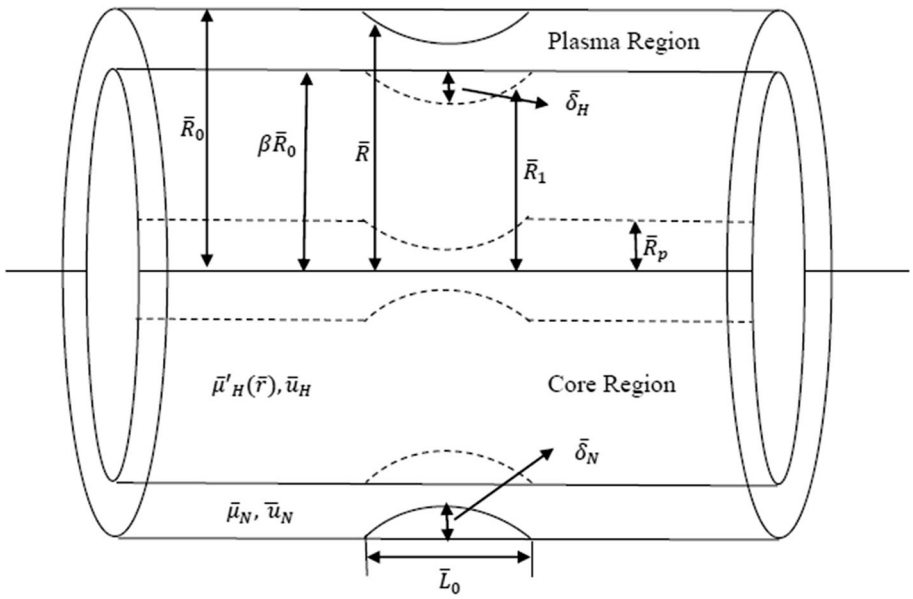

FIGURE 1. The physical sketch of constricted blood vessel for two-fluid model.

The geometry of the blood vessels with time-dependent constrictions in the core and peripheral region are given by Misra *et al.*,[19] Nagarani and Sarojamma,[21] and Sankar and Ismail.[30]

$$\bar{R}_1(\bar{t},\bar{z}) = \begin{cases} \beta\bar{R}_0 - \bar{\delta}_H(1-e^{-\bar{t}\bar{\omega}})\left(1+\cos\frac{\pi\bar{z}}{2\bar{z}_0}\right); & -2\bar{z}_0 \le \bar{z} \le 2\bar{z}_0 \\ \beta\bar{R}_0; & \text{otherwise} \end{cases} \tag{4a}$$

$$\bar{R}(\bar{t},\bar{z}) = \begin{cases} \bar{R}_0 - \bar{\delta}_N(1-e^{-\bar{t}\bar{\omega}})\left(1+\cos\frac{\pi\bar{z}}{2\bar{z}_0}\right); & -2\bar{z}_0 \le \bar{z} \le 2\bar{z}_0 \\ \bar{R}_0; & \text{otherwise} \end{cases} \tag{4b}$$

where $\bar{L}_0 \equiv 4\bar{z}_0$ is the length of the stenotic region; $\bar{\delta}_H$ and $\bar{\delta}_N$ are the maximum height of the stenosis in core region and plasma region, respectively; $\bar{R}_1(\bar{t},\bar{z})$, $\bar{R}(\bar{t},\bar{z})$ are radii of the constricted artery with core and peripheral region, respectively; $\bar{R}_0, \beta\bar{R}_0$ represent the radii of the cell free region and core region for unstenosed artery, respectively and β is the fraction of the core radius to the radius of normal artery.

To solve the above system of nonlinear partial differential equations, the following non-dimensional variables are introduced

$$\tau_H = \frac{\bar{\tau}_H\bar{R}_0}{U_0\bar{\mu}_N}, \quad \tau_N = \frac{\bar{\tau}_N\bar{R}_0}{U_0\bar{\mu}_N}, \quad z_0 = \frac{\bar{z}_0}{\bar{R}_0}, \quad L = \frac{\bar{L}}{\bar{R}_0},$$
$$R_p = \frac{\bar{R}_p}{\bar{R}_0}, \quad p = \frac{\bar{p}\bar{R}_0}{U_0\bar{\mu}_N}, \quad r = \frac{\bar{r}}{\bar{R}_0}, \quad z = \frac{\bar{z}}{\bar{R}_0}, \quad t = \bar{t}\bar{\omega},$$
$$L_0 = \frac{\bar{L}_0}{\bar{R}_0}, \quad \alpha^2 = \frac{\bar{R}_0^2\bar{\omega}\bar{\rho}_N}{\bar{\mu}_N}, \quad \rho_0 = \frac{\bar{\rho}_N}{\bar{\rho}_H}, \quad u_H = \frac{\bar{u}_H}{U_0}, \quad u_N = \frac{\bar{u}_N}{U_0},$$
$$\theta = \frac{\bar{\tau}_y\bar{R}_0}{U_0\bar{\mu}_N}, \quad \delta_H = \frac{\bar{\delta}_H}{\bar{R}_0}, \quad \delta_N = \frac{\bar{\delta}_N}{\bar{R}_0}, \quad R(z) = \frac{\bar{R}(\bar{z})}{\bar{R}_0},$$
$$R_1(z) = \frac{\bar{R}_1(\bar{z})}{\bar{R}_0}, \quad R(t,z) = \frac{\bar{R}(\bar{t},\bar{z})}{\bar{R}_0}, \quad R_1(t,z) = \frac{\bar{R}_1(\bar{t},\bar{z})}{\bar{R}_0},$$

where $\bar{\mu}_H = \bar{\mu}_N\left(\frac{\bar{R}_0}{U_0\bar{\mu}_N}\right)^{1-n}$; α is the Womersley frequency parameter and ω is the angular frequency of the blood flow.

We have taken here the pressure gradient as the function of z and t. Therefore

$$-\frac{\partial p}{\partial z} = q(z)f(t),$$

where $q(z)$ is the steady state pressure gradient and $f(t) = 1 + A\sin t$, A is the amplitude of the pressure gradient.

Using non-dimensional variables, the system of equations (1)-(4) will become

$$\frac{\alpha^2}{\rho_0}\frac{\partial u_H}{\partial t} = q(z)f(t) - \frac{1}{r}\frac{\partial}{\partial r}(r\tau_H), \tag{5a}$$

$$\alpha^2\frac{\partial u_N}{\partial t} = q(z)f(t) - \frac{1}{r}\frac{\partial}{\partial r}(r\tau_N), \tag{5b}$$

where $q(z)f(t) > 0$ and

$$\tau_H = \theta + \left((1+K-Kr^m)\left(-\frac{\partial u_H}{\partial r}\right)\right)^{1/n}, \quad \text{if } \tau \ge \theta, \quad R_p \le r \le R_1(t,z), \tag{6a}$$

$$\frac{\partial u_H}{\partial r} = 0, \quad \text{if } \tau \le \theta, \quad 0 \le r \le R_p, \tag{6b}$$

$$\tau_N = -\frac{\partial u_N}{\partial r}, \quad R_1(t,z) \le r \le R(t,z). \tag{6c}$$

The boundary conditions in non-dimensional form are given by

$$\begin{aligned} &\tau_H \text{ is finite at } r = 0, \\ &\tau_H = \tau_N,\ u_H = u_N \text{ at } r = R_1(t,z), \\ &u_N = 0 \text{ at } r = R(t,z). \end{aligned} \tag{7}$$

The geometry of the stenosis in core and peripheral regions are given as

$$R_1(t,z) = \begin{cases} \beta - \delta_H(1-e^{-t})\left(1+\cos\frac{\pi z}{2z_0}\right); & -2z_0 \le z \le 2z_0 \\ \beta; & \text{otherwise} \end{cases} \tag{8a}$$

$$R(t,z) = \begin{cases} 1 - \delta_N(1-e^{-t})\left(1+\cos\frac{\pi z}{2z_0}\right); & -2z_0 \le z \le 2z_0 \\ 1; & \text{otherwise} \end{cases} \tag{8b}$$

where $(\bar{\delta}_H/\bar{R}_0) \ll 1$ and $(\bar{\delta}_N/\bar{R}_0) \ll 1$.

The volumetric flow rate $Q(z, t)$ in non-dimensional form is given by Misra *et al.*[19]

$$Q(z,t) = 4\int_0^{R(t,z)} ru(z,r,t)dr. \tag{9}$$

SOLUTION FOR STEADY FLOW

Consider two-dimensional axially symmetric, laminar, steady and fully developed flow of blood through a constricted blood vessel as shown in Fig. 1. For arteries with mild stenosis ($\bar{\delta}_N/\bar{R}_0 \ll 1$, Fig. 1), the radial component of momentum equations will be reduced to $\frac{\partial p}{\partial r} = 0$.[42]

In this case, the governing equations are

$$\frac{d\bar{p}}{d\bar{z}} = -\frac{1}{\bar{r}}\frac{d}{d\bar{r}}(\bar{r}\bar{\tau}_H), \quad 0 \le \bar{r} \le \bar{R}_1(\bar{z}), \tag{10a}$$

$$\frac{d\bar{p}}{d\bar{z}} = -\frac{1}{\bar{r}}\frac{d}{d\bar{r}}(\bar{r}\bar{\tau}_N), \quad \bar{R}_1(\bar{z}) \le \bar{r} \le \bar{R}(\bar{z}), \tag{10b}$$

where $\bar{p}$ denotes pressure; $\bar{\tau}_H$ and $\bar{\tau}_N$ denote the shear stresses of Herschel–Bulkley fluid and Newtonian fluid, respectively. The stress and strain relationship for both the fluids are given by

$$\bar{\tau}_H = \bar{\tau}_y + \left[\bar{\mu}'_H(\bar{r})\left(-\frac{\partial \bar{u}_H}{\partial \bar{r}}\right)\right]^{\frac{1}{n}}, \quad \text{if } \bar{\tau} \ge \bar{\tau}_y, \quad \bar{R}_p \le \bar{r} \le \bar{R}_1(\bar{z}), \tag{11a}$$

$$\frac{\partial \bar{u}_H}{\partial \bar{r}} = 0, \quad \text{if } \bar{\tau} \le \bar{\tau}_y, \quad 0 \le \bar{r} \le \bar{R}_p, \tag{11b}$$

$$\bar{\tau}_N = \bar{\mu}_N\left(-\frac{\partial \bar{u}_N}{\partial \bar{r}}\right), \quad \bar{R}_1(\bar{z}) \le \bar{r} \le \bar{R}(\bar{z}), \tag{11c}$$

where $\bar{\mu}'_H(\bar{r})$ denote the radially varying viscosity in core region which is $\bar{\mu}'_H(\bar{r}) = \bar{\mu}_H\{1 + K - K\left(\frac{\bar{r}}{\bar{R}_0}\right)^m\}$[20,24] and $\bar{\mu}_H, \bar{\mu}_N$ are constant viscosity coefficients in core and plasma region, respectively; $\bar{\tau}_y$ the yield stress; n Herschel–Bulkley fluid parameter; m is the viscosity index and K is constant in viscosity relation.

The pressure gradient is assumed as

$$-\frac{dp}{dz} = p_s, \tag{12}$$

where p_s is the non-dimensional steady state pressure gradient.

The governing equations in non-dimensional form are

$$p_s = \frac{1}{r}\frac{d}{dr}(r\tau_H), \quad 0 \le r \le R_1(z), \tag{13a}$$

$$p_s = \frac{1}{r}\frac{d}{dr}(r\tau_N), \quad R_1(z) \le r \le R(z), \tag{13b}$$

and the Eq. (11) in non-dimensional form are given by

$$-\frac{\partial u_H}{\partial r} = \frac{\tau_H^{n-1}(\tau_H - n\theta)}{1 + K - Kr^m}, \quad \tau_H \ge \theta, \quad R_p \le r \le R_1(z), \tag{14a}$$

$$\frac{\partial u_H}{\partial r} = 0, \quad \tau_H \le \theta, \quad 0 \le r \le R_p, \tag{14b}$$

$$-\frac{\partial u_N}{\partial r} = \tau_N, \quad R_1(z) \le r \le R(z), \tag{14c}$$

where $\theta = \frac{\bar{R}_0\bar{\tau}_y}{\bar{\mu}_N U_0}$ is the non-dimensional yield stress.

The non-dimensional form of the boundary conditions are given as

$$\begin{aligned} &\tau_H \text{ is finite at } r = 0, \\ &\tau_H = \tau_N,\ u_H = u_N \text{ at } r = R_1(z), \\ &u_N = 0 \text{ at } r = R(z). \end{aligned} \tag{15}$$

The denominator of the right hand side of Eq. (14a) has been expanded binomially up to third order approximation.[20] Solving Eqs. (13) and (14) and using boundary conditions (15), we obtain

$$\tau_H = \frac{p_s r}{2}, \quad \tau_N = \frac{p_s r}{2}, \tag{16a}$$

$$\begin{aligned} u_H = {} & \frac{p_s}{4}(R^2 - R_1^2) - \frac{2^{-n}(p_s r)^n}{p_s(K+1)} \\ & \left(\frac{p_s r}{n+1} + \frac{K^3 r^{3m}}{(K+1)^3}\left(\frac{p_s r}{3m+n+1} - \frac{2\theta n}{3m+n}\right)\right. \\ & + \frac{K^2 r^{2m}}{(K+1)^2}\left(\frac{p_s r}{2m+n+1} - \frac{2\theta n}{2m+n}\right) \\ & + \frac{Kr^m}{K+1}\left(\frac{p_s r}{m+n+1} - \frac{2\theta n}{m+n}\right) - 2\theta) \\ & + \frac{2^{-n}(p_s R_1)^n}{p_s(K+1)}\left(\frac{p_s}{n+1} - 2\theta\right. \\ & + \frac{K^3 R_1^{3m}}{(K+1)^3}\left(\frac{p_s R_1}{3m+n+1} - \frac{2\theta n}{3m+n}\right) \\ & + \frac{K^2 R_1^{2m}}{(K+1)^2}\left(\frac{p_s R_1}{2m+n+1} - \frac{2\theta n}{2m+n}\right) \\ & \left. + \frac{KR_1^m}{K+1}\left(\frac{p_s R_1}{m+n+1} - \frac{2\theta n}{m+n}\right)\right), \end{aligned} \tag{16b}$$

$$u_N = \frac{p_s}{4}(R^2 - r^2). \tag{16c}$$

We can obtain the plug core velocity from the Eq. (16b) by putting $r = R_p$

$$u_p = u_H \text{ at } r = R_p, \tag{16d}$$

where R_p is the plug core (flow) radius.

The geometry of the stenosis for steady state flow in non-dimensional form is given by

$$R_1(z) = \begin{cases} \beta - \delta_H\left(1 + \cos\frac{\pi z}{2z_0}\right); & -2z_0 \le z \le 2z_0 \\ \beta; & \text{otherwise} \end{cases} \tag{17a}$$

$$R(z) = \begin{cases} 1 - \delta_N\left(1 + \cos\frac{\pi z}{2z_0}\right); & -2z_0 \le z \le 2z_0 \\ 1; & \text{otherwise} \end{cases} \tag{17b}$$

where $R(z)$ and R_0 are the radius of the artery with and without stenosis, respectively.

The volumetric flow rate Q_s in non-dimensional form is given by Sankar and Hemalatha[29]

$$Q_s = 8\int_0^{R(z)} ru(z,r)dr, \\ = 8\left(u_p(z,R_p)\int_0^{R_p} rdr + \int_{R_p}^{R_1(z)} ru_H(z,r)dr + \int_{R_1(z)}^{R(z)} ru_N(z,r)dr\right). \tag{18}$$

The frictional resistance λ_s is given by

$$\lambda_s = \frac{p_s L}{Q_s}, \tag{19}$$

where L is the length of the blood vessel.

SOLUTION FOR PULSATILE FLOW

Using regular perturbation method, the velocity distribution u_H and the shear stress τ_H are assumed to perturbation series form[22]

$$u_H(z,r,t) = u_{H0}(z,r,t) + \alpha^2 u_{H1}(z,r,t) + \cdots, \tag{20a}$$

$$\tau_H(z,r,t) = \tau_{H0}(z,r,t) + \alpha^2 \tau_{H1}(z,r,t) + \cdots, \tag{20b}$$

Similarly, the expressions for velocity, stress for Newtonian fluid and plug core radius for non-Newtonian fluid can also be written in powers of α^2, where $\alpha(\ll 1.0)$ is the Womersley frequency parameter. Here α^2 is being used as perturbation parameter as it depends upon the characteristic velocity.[26]

The non-dimensional form of boundary conditions are given by

$$\tau_{H0} \text{ and } \tau_{H1} \text{ are finite at } r=0, \\ \tau_{H0}=\tau_{N0},\ \tau_{H1}=\tau_{N1},\ u_{H0}=u_{N0},\ u_{H1}=u_{N1} \text{ at } r=R_1(t,z), \\ u_{N0}=u_{N1}=0 \text{ at } r=R(t,z). \tag{21}$$

Putting the values of $u_H(z,r,t)$ and $\tau_H(z,r,t)$ in Eqs. (5) and (6) and equating the coefficients of α^0, we have

$$\frac{\partial}{\partial r}(r\tau_{H0}) = rq(z)f(t), \tag{22a}$$

$$\frac{\partial u_{H0}}{\partial r} = -\frac{\tau_{H0}^{n-1}(\tau_{H0}-n\theta)}{1+K-Kr^m}. \tag{22b}$$

The denominator of the right hand side of Eq. (22b) has been expanded binomially up to third order approximation.[20] Solving Eqs. (22a) and (22b) and using boundary conditions (21), we obtain

$$\tau_{H0} = rq(z)f(t)/2, \tag{23a}$$

$$u_{H0} = \frac{2^{-n}R_1(f(t)q(z)R_1)^{n-1}}{K+1} \\ \times\left(\frac{f(t)q(z)R_1}{n+1} + \frac{K^3R_1^{3m}}{(K+1)^3} \right. \\ \times\left(\frac{f(t)q(z)R_1}{3m+n+1} - \frac{2\theta n}{3m+n}\right) \\ + \frac{K^2R_1^{2m}}{(K+1)^2}\left(\frac{f(t)q(z)R_1}{2m+n+1} - \frac{2\theta n}{2m+n}\right) \\ \left. + \frac{KR_1^m}{K+1}\left(\frac{f(t)q(z)R_1}{m+n+1} - \frac{2\theta n}{m+n}\right) - 2\theta\right) \\ - \frac{2^{-n}r(rf(t)q(z))^{n-1}}{K+1}\left(\frac{rf(t)q(z)}{n+1} + \frac{K^3r^{3m}}{(K+1)^3}\left(\frac{rf(t)q(z)}{3m+n+1}\right.\right. \\ \left. - \frac{2\theta n}{3m+n}) + \frac{K^2r^{2m}}{(K+1)^2}\left(\frac{rf(t)q(z)}{2m+n+1} - \frac{2\theta n}{2m+n}\right)\right. \\ \left. + \frac{Kr^m}{K+1}\left(\frac{rf(t)q(z)}{m+n+1} - \frac{2\theta n}{m+n}\right) - 2\theta\right) + \frac{f(t)q(z)}{4}(R^2-R_1^2). \tag{23b}$$

Using perturbation series expansion, we have

$$\frac{\partial}{\partial r}(r\tau_{N0}) = rq(z)f(t), \tag{24a}$$

$$\frac{\partial u_{N0}}{\partial r} = -\tau_{N0}. \tag{24b}$$

Solving Eqs. (24a) and (24b) and using boundary conditions (21), we have

$$\tau_{N0} = rq(z)f(t)/2, \tag{25a}$$

$$u_{N0} = \frac{f(t)q(z)}{4}(R^2-r^2). \tag{25b}$$

The zeroth-order approximation of plug core velocity can be obtained from the expression of Eq. (23b) as

$$u_{p0} = u_{H0} \text{ at } r = R_{p0}, \tag{26}$$

here R_{p0} is the zeroth order approximation of plug core radius. Similarly, equating the coefficients of α^2 in the Eqs. (5) and (6), we have

$$\frac{1}{\rho_0}\frac{\partial u_{H0}}{\partial t} = -\frac{1}{r}\frac{\partial}{\partial r}(r\tau_{H1}), \tag{27a}$$

$$-\frac{\partial u_{H1}}{\partial r} = \frac{n\tau_{H0}^{n-2}\tau_{H1}(\tau_{H0}-(n-1)\theta)}{1+K-Kr^m}. \tag{27b}$$

The denominator of the right hand side of Eq. (27b) has been expanded binomially up to third order approximation.[20] Similarly, equating the coefficients of α^2 in the Eqs. (5) and (6), we have

$$\frac{\partial u_{N0}}{\partial t} = -\frac{1}{r}\frac{\partial}{\partial r}(r\tau_{N1}), \tag{28a}$$

$$-\frac{\partial u_{N1}}{\partial r} = \tau_{N1}. \tag{28b}$$

The wall shear stress τ_w can be obtained as

$$\tau_w = \left(\tau_{N0} + \alpha^2 \tau_{N1}\right)_{r=R}. \tag{29}$$

The shear stress $|\tau_H| = (|\tau_{H0}| + \alpha^2|\tau_{H1}|)$ at $r = R_p$ is given by

$$(|\tau_{H0}| + \alpha^2|\tau_{H1}|) = \theta \text{ at } r = R_p. \tag{30}$$

Using Taylor's series expansion of τ_{H0} and τ_{H1} about R_{p0} and using $|\tau_{H0}(R_{p0})| = \theta$, we have

$$R_{p1} = \frac{-|\tau_{H1}(R_{p0})|}{q(z)f(t)}. \tag{31}$$

The flow resistance λ is defined as

$$\lambda = \frac{p_0 - p_L}{Q(z,t)}, \tag{32}$$

where pressure $p = p_0$ at $z = 0$ and $p = p_L$ at $z = L$.

The solution of Eqs. (27a,27b) and (28a,28b) for u_{H1} and u_{N1} with help of Eqs. (23a, 23b) and (25a,25b) by using the boundary conditions (21) are obtained by Mathematica Software but due to very large expressions it has not been mentioned here. Therefore the mathematical expression for the first order approximation u_{H1}, u_{N1} and Q, λ, τ_w have not been mentioned in the manuscript.

RESULTS AND DISCUSSION

A comparative study between single and two-fluid model has been done in the present section and the effect of varying nature of viscosity on fluid flow quantities such as plug flow (core) velocity u_p, flow rate Q, wall shear stress τ_w and flow resistance λ are graphically analyzed and compared with constant viscosity model. This model identifies the Newtonian fluid if yield stress $\theta = 0$ and $n = 1$, Bingham-plastic fluid if $\theta \neq 0$ and $n = 1$, a Power-law fluid if $\theta = 0$ and $n \neq 1$ and in case of Herschel–Bulkley fluid, we have taken here a specific value of yield stress as $\theta \neq 0$ (0.05) and the value of the Power-law index as $n \neq 1$ (1.05). These values are used for a comparative analysis of some hemodynamical quantities for four fluids (NF, PL, BP, HB as fluid in core region, respectively). The value of Herschel–Bulkley fluid parameter (or Power-law index) n for blood flow models is taken as 0.95 when $n < 1$ and 1.05 when $n > 1$.[28] The range of value of K lies between 0.0–0.9 as per suggestion of Misra and Ghosh.[20] The value of the density ratio ρ_0 is taken as unity throughout the analysis. The value of viscosity index varies from 0–10 for steady flow and pulsatile flow situation. The typical value of the $p_s = 1$ for steady state[29] and $q(z) = 1$ for pulsatile state.[21] Following Shukla *et al.*,[36] relations $R_1 = \beta R$ and $\delta_H = \beta\delta_N$ are used to calculate R_1 and δ_H. When $\beta = 1$, the two-fluid model reduced to single-fluid model (Herschel–Bulkley fluid model). This model reduces to constant viscosity model, if we choose either the viscosity parameter $K = 0$ or viscosity index $m = 0$.

Steady Flow

First of all we would emphasize upon the areas in which our model agrees with previously established constant viscosity models (either viscosity parameter $K = 0$ or viscosity index $m = 0$) for steady flow involving single as well as two-fluid models. The details are as follows:

(1) The velocity distribution decreases radially with parabolic profile and slightly flattened near the axis due to presence of yield plane location under constant as well as varying viscosity assumption (Fig. 2).
(2) Like the previously established constant viscosity model, here also plug flow velocity and flow rate decays with increasing yield stress (Figs. 3 and 4a) and height of stenosis (Figs. 3 and 4b) for single as well as two-fluid model.
(3) Analysis of flow rate with yield stress for different peripheral layer thickness and different values of viscosity index reveals that flow rate assumes slightly higher values with increase in peripheral layer thickness (i.e., reduced β) (Fig. 4a). This result is in good agreement with Srivastava and Saxena.[40]
(4) Like the previous studies for constant viscosity model, here also the flow rate assumes relatively higher values for two-fluid model in comparison to single-fluid model and

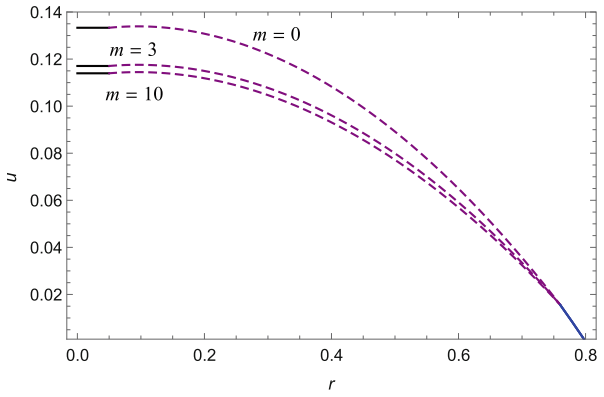

FIGURE 2. Variation of velocity profile u with radial distance r in steady flow for different values of m. ($z = 0, \theta = 0.05, K = 0.2, p_s = 1, \delta_N = 0.1, \beta = n = 0.95$).

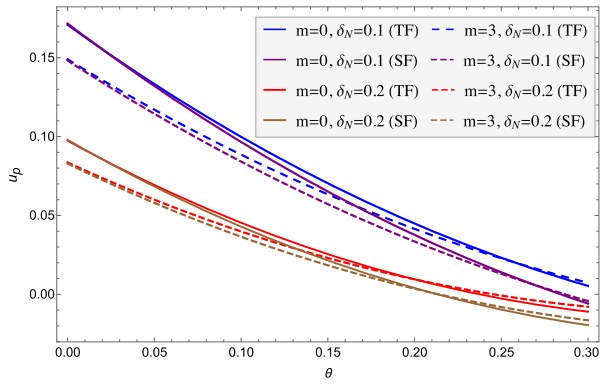

FIGURE 3. Variation of plug core velocity u_p with yield stress θ for different values of viscosity index m and height of constriction δ_N. ($K = 0.2, p_s = 1, z = 0, n = 0.95$).

increases with rising pressure gradient (Fig. 5).

(5) In agreement with the previous studies, the flow resistance in our formulation increases with yield stress (Fig. 6a) and height of stenosis (Fig. 6b) and it assumes lesser value for two-fluid model in comparison to single-fluid model.

(6) From Fig. 6a, the analysis of flow resistance with yield stress for different peripheral layer thickness and different values of viscosity index divulge that flow resistance assumes slightly lesser values with increase in peripheral layer thickness (i.e., reduced β). This result is in good agreement with Srivastava and Saxena.[40]

Now we present the new observations emphasizing the effect of varying viscosity (viscosity parameter $K \neq 0$ and viscosity index $m \neq 0$) on various hemodynamical quantities such as velocity profile, plug flow velocity, wall shear stress, flow rate and flow resistance. The details are as follows:

- For rising viscosity index (m), the following observations have been made:

(1) From Fig. 2, it is pointed out that velocity is slightly reduced for higher viscosity index and there is no varying viscosity effect in peripheral region i.e., curves are almost coincide for different viscosity indexes. This signifies the effect of varying nature of viscosity.

(2) A rising viscosity index leads to decay in plug flow velocity. The plug flow velocity becomes higher for two-fluid model in comparison with single-fluid model which is in resemblance with the practical situations (Fig. 3). The decay rate of plug flow velocity

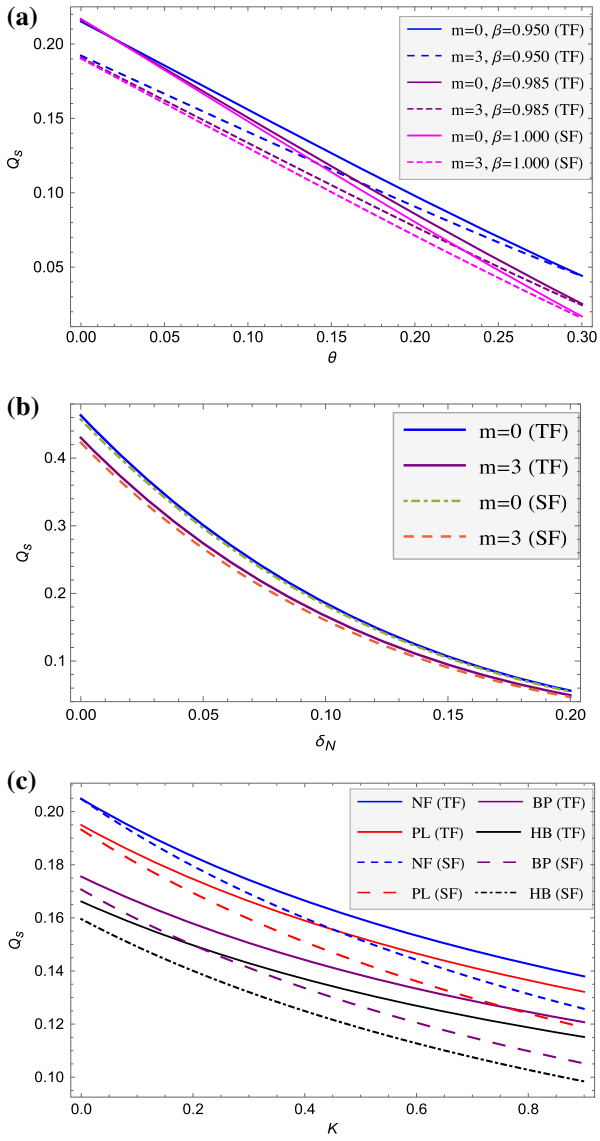

FIGURE 4. Variation of flow rate Q_s with (a) yield stress θ ($K = 0.2, \delta_N = 0.1$), (b) height of constriction δ_N ($K = 0.2, \theta = 0.05$), (c) viscosity parameter K for different values of viscosity index m and β . ($p_s = 1, z = 0, n = 0.95$).

with yield stress reduces with rising viscosity index.

(3) From Fig. 3, a noteworthy observation is that the difference in plug flow velocity for single and two-fluid model is slightly increased for higher viscosity index in comparison to constant viscosity model which shows that the velocity in plug flow region is affected by varying nature of viscosity for two-fluid model.

(4) From Fig. 5, an important observation is that the difference in flow rate for single and two-fluid model is slightly higher for higher viscosity index emphasizing the effect of

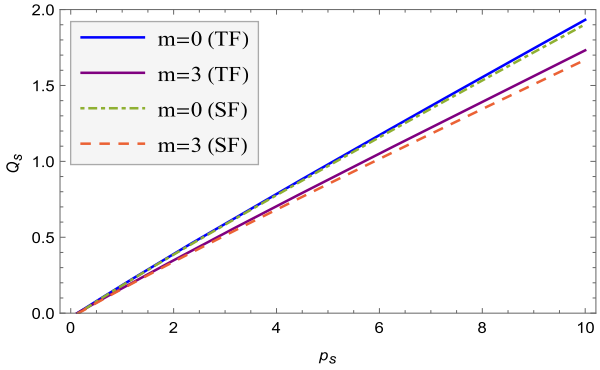

FIGURE 5. Variation of flow rate Q_S with pressure gradient p_S in steady flow for different values of viscosity index m. ($K = 0.2, \theta = 0.05, z = 0, \delta_N = 0.1, n = 0.95$).

varying viscosity on flow rate in two-fluid model.

(5) An interesting observation is that the variable nature of viscosity leads to relatively higher change in flow resistance for two-fluid model in comparison to single-fluid model (Fig. 6b). Hence we can conclude that the variable nature of viscosity leads to changes in flow resistance, but the magnitude up to which the flow resistance changes depends upon the nature of blood vessels (i.e., stenotic region as the difference increases with height of stenosis).

- Under varying viscosity assumption, the rising yield stress leads to the following observations:

(1) From Fig. 3, the effect of varying viscosity on plug flow velocity is diminished for higher yield stress (approximately $\theta = 0.25$ when $\delta_N = 0.1$) and this stage is attained at lesser value of yield stress θ when height of stenosis δ_N increases (approximately $\theta = 0.20$ when $\delta_N = 0.2$).

(2) A rising viscosity index leads to further decay in flow rate with yield stress for single as well as two-fluid model (Fig. 4a). The decay rate for variation of flow rate with yield stress is reduced for higher viscosity index. It is also noted that the decay rate of flow rate with yield stress is higher for single-fluid model in comparison to two-fluid model under varying viscosity assumption.

(3) An enhanced flow resistance with yield stress is found for single as well as two-fluid model with varying viscosity assumption (Fig. 6a). Here also we observed a weak effect of varying viscosity on flow resistance for two-fluid model at high yield stress as the difference in flow resistance for two-fluid model is very small between constant and varying viscosity approaches. It is also seen that the difference in flow resistance between constant and varying viscosity approaches was significant even at higher yield stress for single-fluid model.

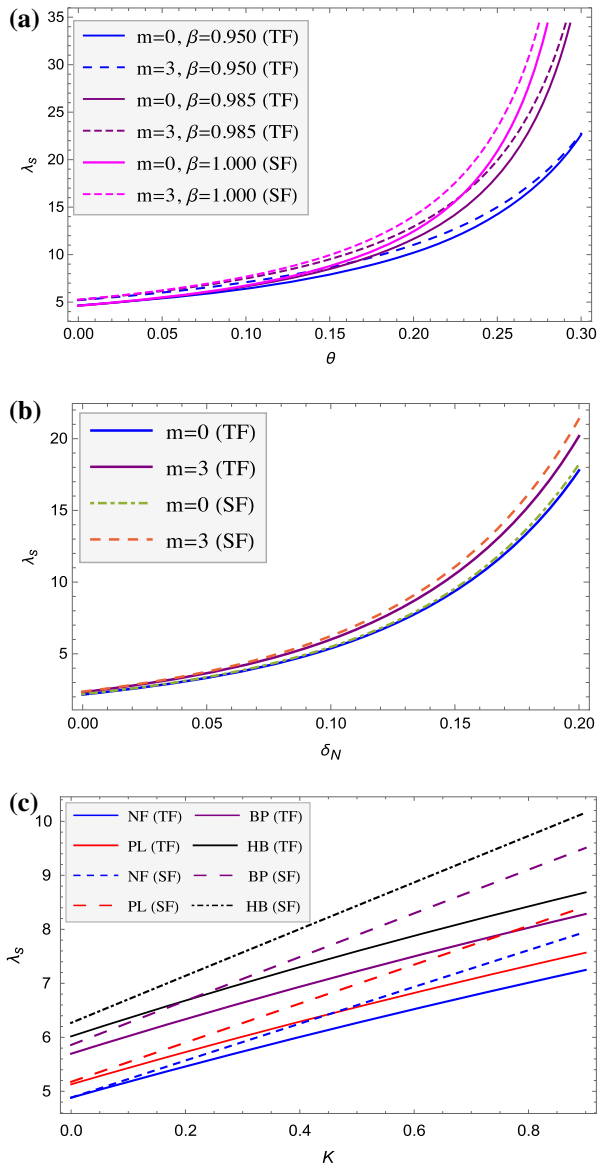

FIGURE 6. Variation of flow resistance λ_S with (a) yield stress θ ($K = 0.2, \delta_N = 0.1$), (b) height of constriction δ_N ($K = 0.2, \theta = 0.05$), (c) viscosity parameter K ($\delta_N = 0.1$) for different values of viscosity index m and β. ($p_s = 1, z = 0, n = 0.95$).

- Under varying viscosity assumption, the rising height of stenosis leads to the following observations:

(1) From Fig. 4b, a remarkable observation is that the difference in flow rate with height of

stenosis for single and two-fluid model is slightly increased for higher viscosity index in comparison to constant viscosity model which shows that the flow rate is affected by varying nature of viscosity for two-fluid model. However, at higher δ_N ($\delta_N \approx 0.2$) the difference is almost negligible.

(2) Another significant observation is that the difference in flow resistance between single and two-fluid model is more significant for higher viscosity index and higher height of stenosis, despite the fact that the yield stress is low (Fig. 6b). Hence this emphasize that varying nature of viscosity leads to significant change in flow resistance in narrowed artery even at low yield stress for two-fluid model.

- The effect of peripheral layer thickness under varying viscosity assumption leads to the following observations:

(1) Figure 4a depicts that flow rate decreases with yield stress for rising viscosity index under different peripheral layer thickness however a reduced peripheral layer thickness leads to rise in decay rate of flow rate with yield stress.

(2) Figure 6a shows that flow resistance increases with rising viscosity index under different peripheral layer thickness but this growth rate is lesser for higher peripheral layer thickness. However, different peripheral layer thickness agrees to diminished effect of varying viscosity at higher yield stress.

- The effect of viscosity parameter (K) under varying viscosity index (m) leads to the following observations:

(1) Figure 4c demonstrates the effect of viscosity parameter K on variation of flow rate for different four fluids (Newtonian fluid-NF, Bingham-plastic fluid-BP, Power-law fluid-PL and Herschel–Bulkley fluid-HB). It is clear that flow rate decreases with increase in viscosity parameter K for single as well as two-fluid model. An important observation is that the value of flow rate is maximum for Newtonian fluid and least for Herschel–Bulkley fluid for single as well as two-fluid model under varying viscosity assumption. Decay rate of flow rate increases for single-fluid model in comparison to two-fluid model and this difference gradually increases from NF to HB fluid, showing the significant impact of varying viscosity on flow rate.

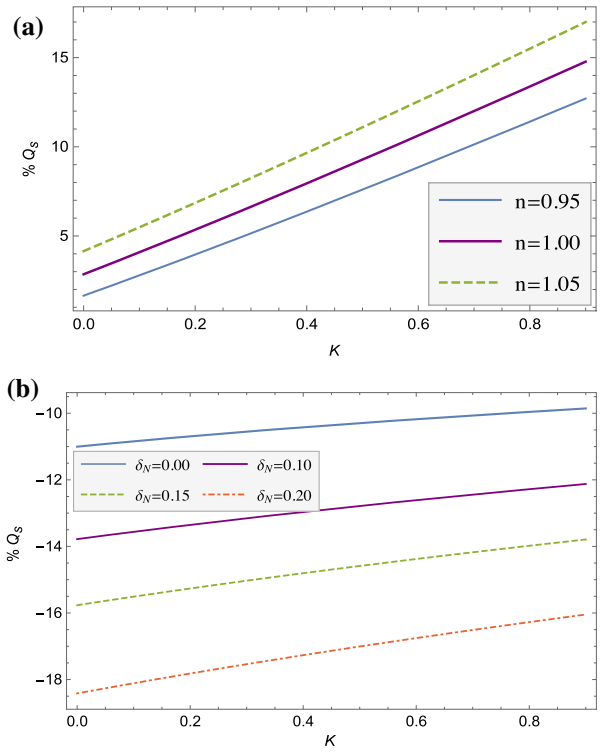

FIGURE 7. % variation of flow rate Q_s with viscosity parameter K (a) b/w single and two-fluid model for different n ($\delta_N = 0.1$), (b) b/w non-Newtonian and Newtonian fluid for different δ_N ($n = 0.95$). ($m = 3, z = 0, \beta = 0.95, p_s = 1$).

(2) Figure 7a presents the relative variation (in percentage) of flow rate with viscosity parameter K between single and two-fluid model for different values of HB fluid parameter n. It is clear that relative variation in flow rate between single and two-fluid models increases with increase in the value of viscosity parameter K and HB fluid parameter n as well. Larger value of viscosity parameter K leads to significant variation in flow rate of two-fluid model relative to single-fluid model. This shows that larger viscosity parameter K significantly distinguishes two-fluid model with single-fluid model.

(3) Figure 7b depicts the relative variation (in percentage) of flow rate with viscosity parameter K between non-Newtonian and Newtonian fluid (as a core region fluid) under different height of stenosis δ_N. The relative difference in flow rate increases more rapidly with respect to viscosity parameter K in constricted blood vessel in comparison to blood vessel without constriction.

(4) The effect of viscosity parameter K on variation of flow resistance for different four

fluids (Newtonian fluid-NF, Bingham-plastic fluid-BP, Power-law fluid-PL and Herschel–Bulkley fluid-HB) is demonstrated in Fig. 6c. It is clear that flow resistance increases with increase in viscosity parameter K for single as well as two-fluid model. An important observation is that the value of flow resistance is maximum for HB fluid and least for Newtonian fluid for single as well as two-fluid model under varying viscosity assumption. The growth rate for flow resistance increases from two-fluid model to single-fluid model and this rise further increases from NF to HB fluid. It is also observed that viscosity parameter K is more effective as we move from NF to HB fluid.

(5) Figure 8a presents the relative variation (in percentage) of flow resistance with viscosity parameter K between single and two-fluid model for different values of HB fluid parameter n. It is clear that percentage variation decreases with increase in viscosity parameter K and HB fluid parameter n as well. Larger value of viscosity parameter K leads to significant variation in flow resistance of two-fluid model relative to single-fluid model. This shows that larger viscosity parameter K significantly distinguishes two-fluid model with single fluid model. The rate at which this change takes place, increases with rise in HB fluid parameter n showing that viscosity parameter K is less effective for shear-thickening fluids $(n<1)$ than shear-thinning fluids $(n>1)$.

(6) Figure 8b depicts the relative variation (in percentage) of flow resistance with viscosity parameter K between non-Newtonian and Newtonian fluid (as a core region fluid) under different height of stenosis δ_N. It is observed that percentage variation reduces with increasing value of viscosity parameter K and it attains significantly higher values for larger height of stenosis. The relative difference in flow resistance decreases more rapidly with respect to viscosity parameter K in constricted blood vessel in comparison to blood vessel without constriction.

Pulsatile Flow

Like the steady flow case in the previous sub-section, here also we present the similarity of our model with constant viscosity model for pulsatile flow as follows:

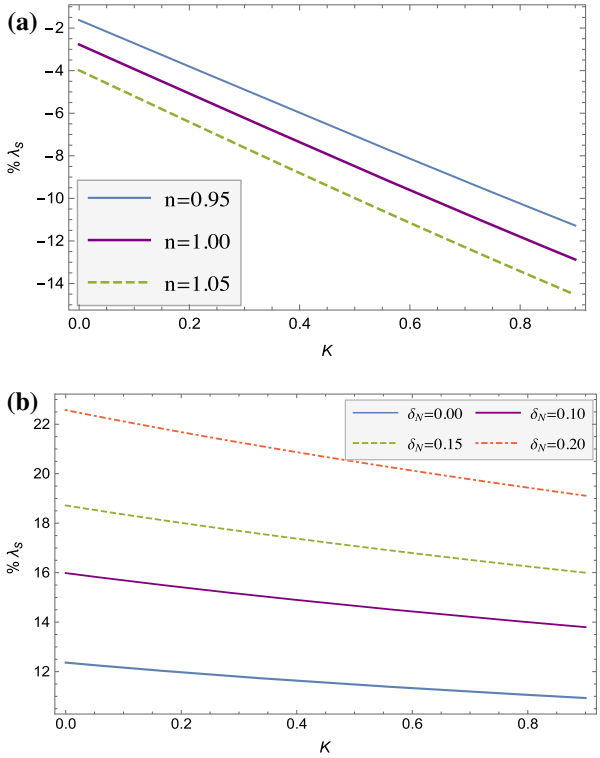

FIGURE 8. % variation of flow resistance λ_s with viscosity parameter K (a) b/w single and two-fluid model for different n ($\delta_N = 0.1$), (b) b/w non-Newtonian and Newtonian fluid for different δ_N ($n = 0.95$). ($m = 3, z = 0, \beta = 0.95, p_s = 1$).

(1) Like the steady flow analysis, velocity distribution also decreases radially with parabolic profile and slightly flattened near the axis within the yield plane location due to presence of yield stress under constant as well as varying viscosity assumption (Fig. 9).

(2) Figure 10 shows the plug flow radius is constant with axial distance for unstenosed artery while plug flow radius decreases gradually from $z = -2.0$ to $z = 0.0$ and increases gradually from $z = 0.0$ to $z = 2.0$ for constricted artery and the decay rate become higher for larger height of stenosis which is in good agreement with the previous works involving constant viscosity approach.

(3) For pulsatile flow, plug flow velocity and flow rate decrease with yield stress (Figs. 11 and 14) for different height of stenosis while the flow resistance increases with both (Fig. 17). These variations are in good agreement with the previous studies for pulsatile flow. Figure 12 shows sinusoidal variation of plug flow velocity with time and slightly larger value of plug flow velocity for two-fluid model.

(4) Figure 13 shows the variation of wall shear stress with time under varying viscosity

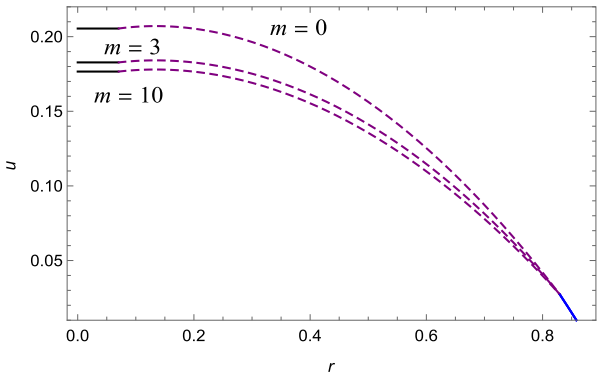

FIGURE 9. Variation of velocity profile u with radial distance r for different values of m. ($A = \alpha = 0.5$, $z = 0, t = 1, \theta = 0.05$, $K = 0.2, \delta_N = 0.1, \beta = n = 0.95$).

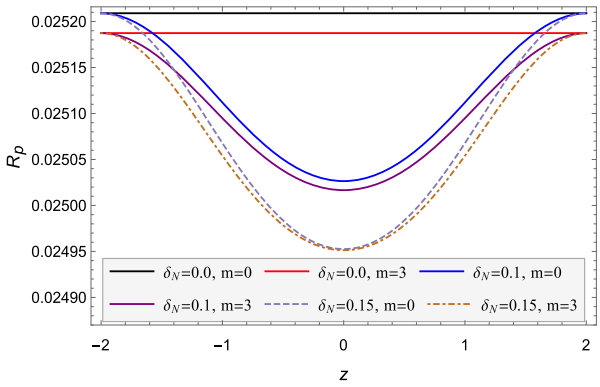

FIGURE 10. Axial variation of plug core radius R_p for different values of δ_N and viscosity index m. ($\theta = 0.05, \alpha = A = 0.5, K = 0.2, t = 1, z_0 = 1, \beta = n = 0.95$).

assumption. We conclude here that the pulsatile nature of wall shear stress remains unchanged under varying viscosity assumption and here also the wall shear stress decays with rising height of stenosis and decreasing pressure gradient amplitude which is in good agreement with the previously established constant viscosity model.

(5) A comparative analysis of variation of flow rate with height of stenosis for all four fluids (NF, PL, BP, HB) shows that the flow rate is maximum for Newtonian fluid and minimum for HB fluid (Fig. 15a) and it assumes slightly higher values for two-fluid model (Fig. 15b) which agrees with previous studies.

(6) From Fig. 16a, flow rate follows periodic variation with time after $t = 3$, which is in good agreement with previous works.[19]

(7) Like the previous studies among four fluids (NF, PL, BP, HB), the flow resistance is minimum for Newtonian fluid and maximum for HB fluid (Fig. 18a) and it assumes slightly lower value for two-fluid model (Fig. 18b) for any value of height of stenosis.

(8) Like previous studies, here also a pulsatile nature of flow resistance with time is observed for higher pressure gradient amplitude (Fig. 19a). Since the stenosis geometry is similar to Shit *et al.*[19] (i.e., the region become narrower with increasing time), so significant increase in flow resistance in the beginning is observed which is on the lines of the results of Shit *et al.*[19]

Following are the new observations on effects of varying viscosity upon various fluid flow quantities such as velocity distribution, plug flow velocity, wall shear stress, flow rate and flow resistance for pulsatile flow situation.

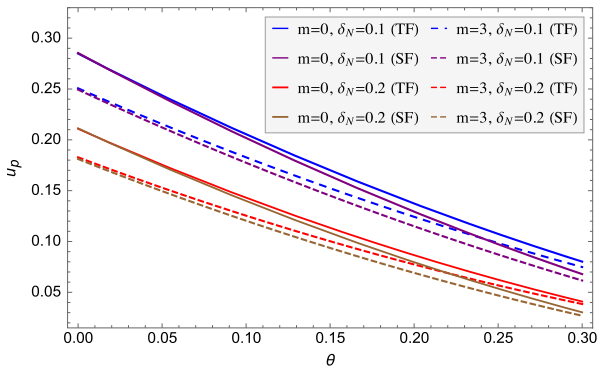

FIGURE 11. Variation of plug core velocity u_p with yield stress θ for different values of viscosity index m and δ_N. ($z = 0$, $t = 1, \alpha = A = 0.5$, $K = 0.2$, $n = 0.95$).

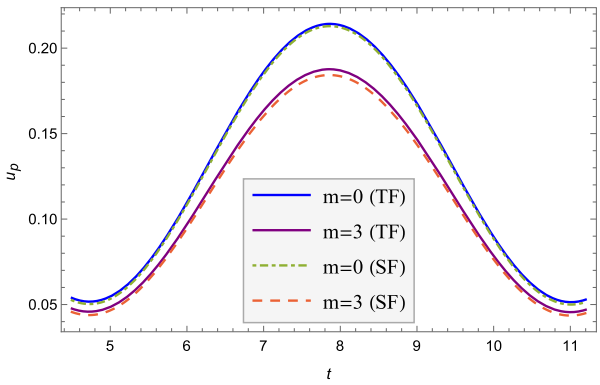

FIGURE 12. Variation of plug core velocity u_p with time t for different values of m at the center of the stenosis. ($\theta = 0.05$, $\alpha = A = 0.5$, $K = 0.2$, $n = 0.95, \delta_N = 0.1$).

- For rising viscosity index (m), the following observations have been made:

(1) Velocity distribution decays with rising viscosity index (Fig. 9). An important observation is that the decay rate become smaller for larger viscosity

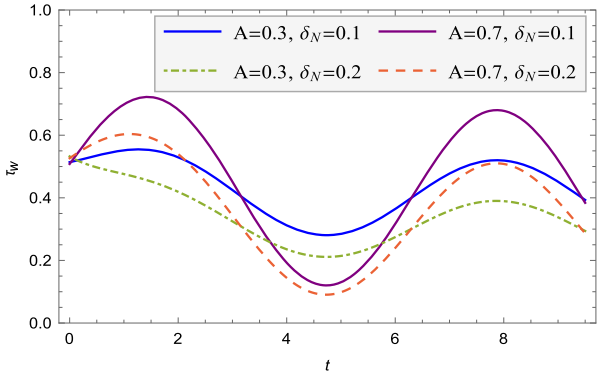

FIGURE 13. Variation of wall shear stress τ_w with time t for different values of δ_N and amplitude of pressure gradient A. ($\beta = n = 0.95$, $m = 3$, $\alpha = 0.5$, $K = 0.2, \theta = 0.05, z = 0$).

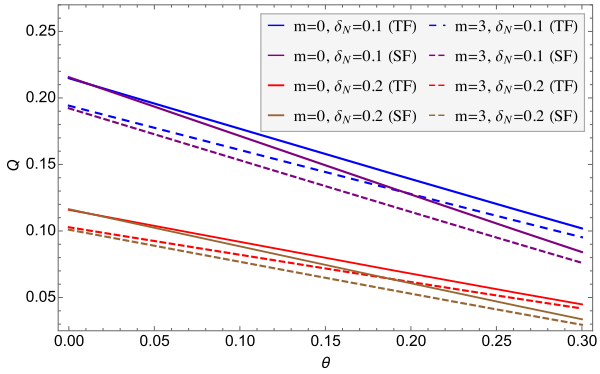

FIGURE 14. Variation of volumetric flow rate Q with yield stress θ for different values of viscosity index m and δ_N. ($K = 0.2, \alpha = A = 0.5, z = 0, n = 0.95, t = 1$).

index and remains unaffected in the peripheral region for larger viscosity index.

(2) Figure 10 shows that the decay rate in plug flow radius with axial distance z become smaller for higher viscosity index. This emphasize the effect of varying viscosity on yield plane location along axial direction in the blood flow through blood vessels. The yield plane location significantly changes for higher viscosity index but this change is almost negligible at the position where the height of stenosis is maximum. Also the shifting in yield plane location for higher viscosity index is maximum for unstenosed arteries.

(3) Slightly reduced values for plug flow velocity with yield stress and height of stenosis (Fig. 11) is observed under varying viscosity assumption.

(4) A sinusoidal variation of plug flow velocity with time is observed in Fig. 12 and here also slight difference is reported for plug flow velocity between single and two-fluid model at higher viscosity index.

(5) For rising viscosity index, the decay rate of flow rate with yield stress is reduced for both single as well as two-fluid model (Fig. 14).

(6) There is more difference in flow rate with height of stenosis between single and two-fluid model for varying nature of viscosity in comparison to constant viscosity model which emphasize the effect of varying nature of viscosity on flow rate (Fig. 14).

(7) Variation of flow rate with height of stenosis is depicted in Fig. 15a for different fluids (NF, PL, BP, HB) and for rising viscosity index flow rate gradually decreases with height of stenosis. An increasing difference between flow rates of single and two-fluid models under varying viscosity assumption is reported in Fig. 15b which is least for Newtonian fluid and most for Herschel–Bulkley fluid.

(8) Figure 16a shows the pulsatile variation of flow rate with time. It is observed that for fixed pressure gradient amplitude the flow rate slightly decays with higher viscosity index. At higher pressure gradient amplitude the flow rate with time for varying viscosity is slightly decreased at the trough but this decay is significant at crest.

(9) An interesting observation is that varying nature of viscosity leads to a relatively higher growth in flow resistance for single-fluid model in comparison to two-fluid model (Fig. 17). The difference in flow resistance between constant and varying viscosity model is relatively very small for two-fluid model in comparison to single-fluid model.

(10) Figure 19a shows the variation of flow resistance with time under varying viscosity assumption and observed a relatively higher flow resistance for higher viscosity index at fixed pressure gradient amplitude.

- Under varying viscosity assumption, the rising yield stress leads to the following observations:

  (1) Figure 11 shows that the decay rate of plug flow velocity with yield stress increases for higher viscosity index which is slightly more in single-fluid model relative to two-fluid model.

  (2) A reduced flow rate is observed under varying viscosity assumption for single as well as two-fluid model (Fig. 14). A diminishing effect of varying viscosity on flow rate

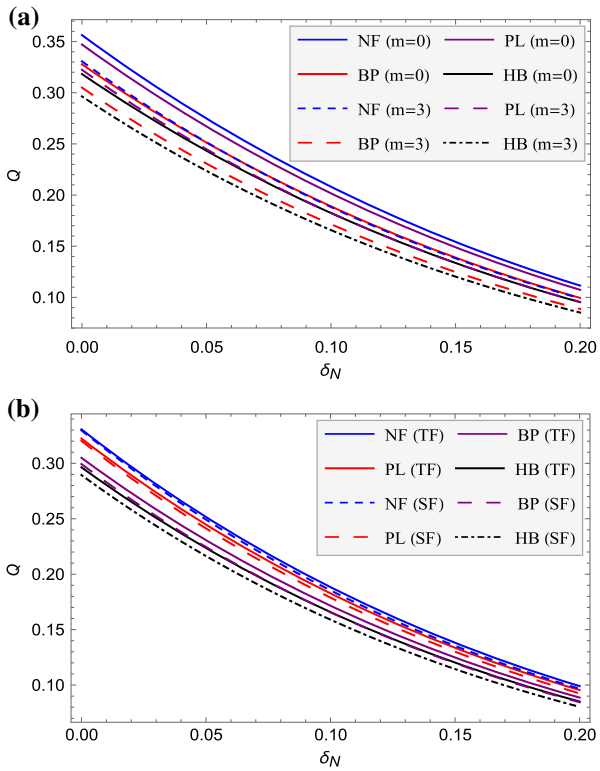

FIGURE 15. Variation of flow rate Q with height of constriction δ_N for different values of (a) viscosity index m ($\beta = 0.95$), (b) plasma layer thickness $(1-\beta)$ ($m = 3$) for different four fluids (NF, BP, PL, HB). ($K = 0.2, A = \alpha = 0.5, z = 0, t = 1$).

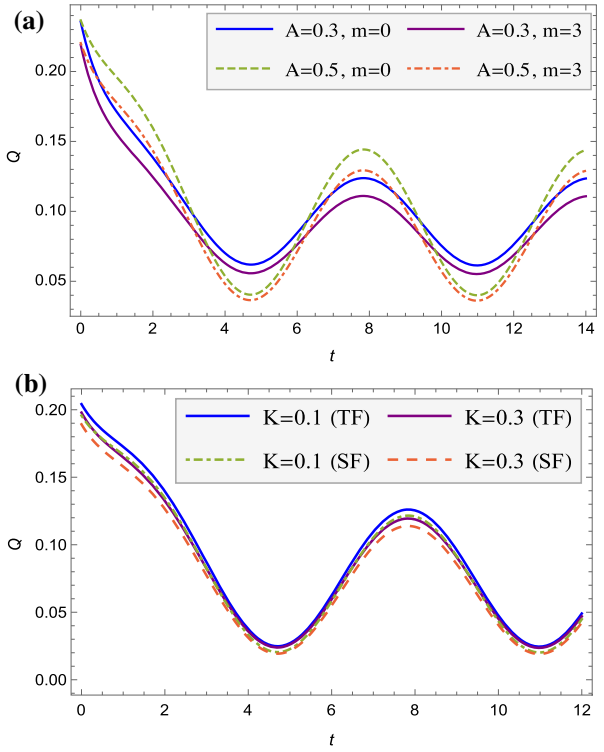

FIGURE 16. Variation of flow rate Q with time t for different (a) viscosity index m and amplitude of pressure gradient A ($K = 0.2, \beta = 0.95$), (b) viscosity parameter K ($m = 1, A = 0.5$). ($n = 0.95, z = 0, \alpha = 0.5, \theta = 0.05, \delta_N = 0.1$).

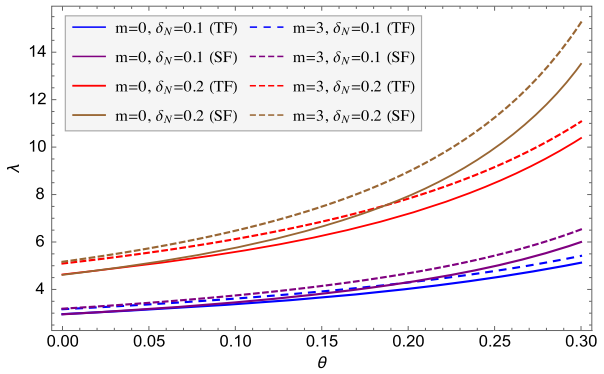

FIGURE 17. Variation of flow resistance λ with yield stress θ for different values of index m and δ_N. ($n = 0.95, \rho_0 = t = 1, K = 0.2, \alpha = A = 0.5, L = 5, z = 0$).

is observed at high yield stress which is more dominant in two-fluid model in comparison to single-fluid model.

- Under varying viscosity assumption, the height of stenosis leads to the following observations:
  (1) A notable observation is that there is more difference between plug flow velocity of single and two-fluid model for varying nature of viscosity in comparison to constant viscosity model (Fig. 11).
  (2) Figure 15a depicts that decay rate of flow rate with height of stenosis is slightly reduced (almost 3%) for all four fluid models under higher viscosity index.
  (3) The varying viscosity is more effective in comparison with constant viscosity approach on variation of flow resistance with height of constriction (Fig. 17). The difference between flow resistance for single and two-fluid model is relatively higher for higher viscosity index.
  (4) For rising viscosity index, growth in flow resistance with height of stenosis is observed in Fig. 18a for different fluids (NF, PL, BP, HB) and the growth rate is more significant at higher height of stenosis.
  (5) Figure 18b presents the variation of flow resistance with height of stenosis under varying viscosity assumption. An increasing difference between flow resistance of single and two-fluid models under varying viscosity assumption is reported which is least for Newtonian fluid and most for Herschel–Bulkley fluid at higher height of stenosis.

- The effect of viscosity parameter (K) under varying viscosity index (m) leads to the following observations:
  (1) The sinusoidal variation of flow rate with time for different values of viscosity parameter K is discussed in Fig. 16b. A significant observation is that for larger values of K the difference between flow rate of single and two-fluid model is relatively more in comparison to flow rate corresponding to the lower values of K at crest. This also emphasize the effect of varying viscosity on flow rate for two-fluid model.
  (2) From Fig. 19b, we observe that the difference in flow resistance between two and single-fluid model is higher for higher viscosity parameter K.
  (3) The relative difference (in percentage) in wall shear stress between two-fluid model and single-fluid model and non-Newtonian and Newtonian fluid models is very small as evident from Tables 1 and 2. This variation remains same for large as well as small viscosity index m.

CONCLUSION

The motivation of this study came from the fact that deposition of fatty plaques leads to narrowing of artery. This constriction may be of any complex geometry and we have considered a shape that is feasible for the analytical treatment of the problem as well as to perform a comparative study with previous models.[21] A comparative study of varying viscosity with constant viscosity model of blood flow through small blood vessels with constriction has been done in the present work. The effect of varying viscosity on velocity profile, plug core velocity, flow rate, flow resistance is analyzed and it is observed that all these quantities are affected by varying nature of viscosity of blood. From the above study, the main findings are pointed out as follows

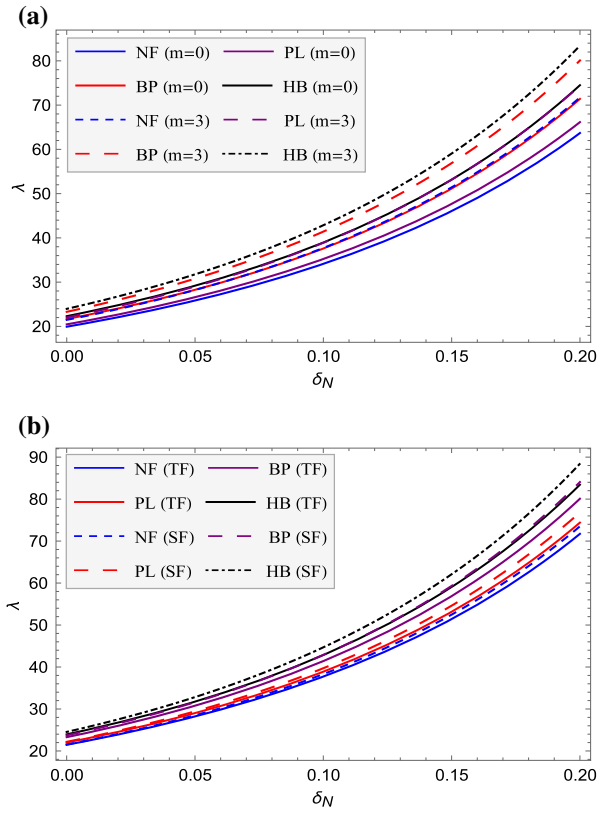

FIGURE 18. Variation of flow resistance λ with height of constriction δ_N for different values of (a) viscosity index m ($\beta = 0.95$), (b) plasma layer thickness $(1-\beta)$ ($m = 3$) for different fluids (NF, BP, PL, HB). ($K = 0.2, A = \alpha = 0.5, L = 5, z = 0, t = 1$).

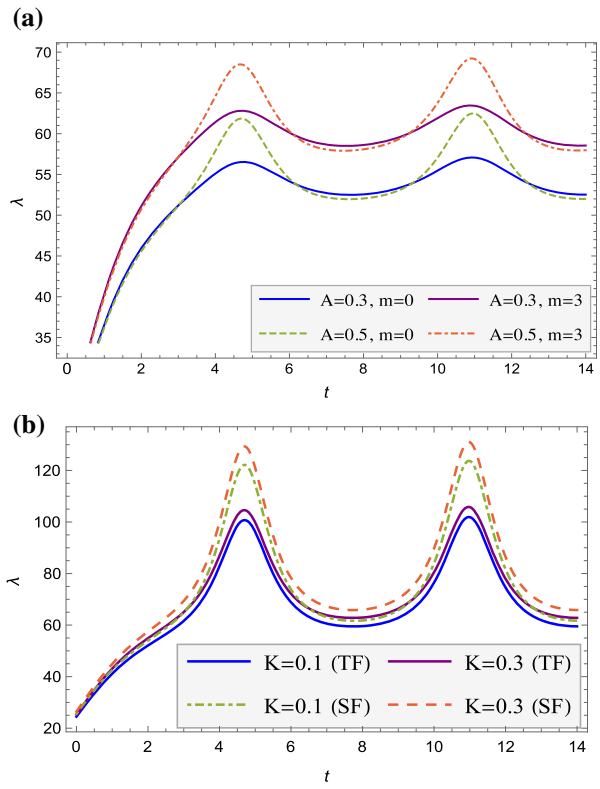

FIGURE 19. Variation of flow resistance λ with time t for different (a) viscosity index m and amplitude of pressure gradient A ($K = 0.2, \beta = 0.95$), (b) viscosity parameter K ($m = 1, A = 0.5$). ($n = 0.95, z = 0, \alpha = 0.5, \theta = 0.05, \delta_N = 0.1, L = 5$).

TABLE 1. Relative variation (in percentage) in wall shear stress τ_w between single and two-fluid model for different values of viscosity index m and viscosity parameter K. ($\theta = 0.05, n = 0.95, \alpha = A = 0.5, \rho_0 = t = 1, \delta_N = 0.1, z = 0$).

	m = 1.0	m = 3.0	m = 7.0	m = 10.0
K = 0.1	− 0.095449	− 0.097277	− 0.096755	− 0.095201
K = 0.3	− 0.098799	− 0.102868	− 0.100187	− 0.096017
K = 0.5	− 0.100961	− 0.106120	− 0.100996	− 0.094909
K = 0.7	− 0.101990	− 0.107626	− 0.100359	− 0.092937
K = 0.9	− 0.102128	− 0.107912	− 0.009893	− 0.090613

TABLE 2. Relative variation (in percentage) in wall shear stress τ_w between non-Newtonian and Newtonian fluid (fluid as in core region) model for different values of viscosity index m and viscosity parameter K. ($\theta = 0.05, n = 0.95, \alpha = A = 0.5, \rho_0 = t = 1, \delta_N = 0.1, z = 0$).

	m = 1.0	m = 3.0	m = 7.0	m = 10.0
K = 0.1	− 0.054784	− 0.053418	− 0.051946	− 0.051404
K = 0.3	− 0.052875	− 0.049275	− 0.045698	− 0.044461
K = 0.5	− 0.050936	− 0.045702	− 0.040793	− 0.039171
K = 0.7	− 0.048965	− 0.042580	− 0.036838	− 0.025006
K = 0.9	− 0.047001	− 0.039829	− 0.033582	− 0.031642

- The varying viscosity effect on flow resistance for two-fluid model is diminished (almost coincide) at higher yield stress which was not the case for single-fluid model. It is also concluded that even for lower yield stress the effect of varying viscosity on flow rate and flow resistance for two-fluid model is almost negligible for larger height of stenosis.
- An important conclusion from this study is that the shift in yield plane location with higher viscosity index for two-fluid model is relatively small in comparison to single-fluid model.
- It is concluded that with increasing viscosity parameter K, the relative percentage variation in various quantities (flow rate Q_s and flow resistance λ_s) significantly changes. This emphasize the effect of varying viscosity on flow through blood vessel with constriction. It is also concluded that the relative difference in flow rate increases more rapidly with respect to viscosity parameter K in constricted blood vessel in comparison to blood vessel without constriction.

Above conclusions lead to significant improvement in accurate measurement of flow rate and flow resistance for modeling of blood flow through constricted blood vessels using two-fluid approach as it takes into account the variable nature of viscosity. This is also important because flow rate and flow resistance is an important parameter to be measured for treatment of atherosclerosis disease. Using constant viscosity for two-fluid model may lead to error in computing flow resistance as it is higher for varying viscosity model. So it is advised to use this model for computing hemodynamic quantities flow rate, flow resistance *etc*. more accurately.

ACKNOWLEDGMENTS

Authors acknowledge their sincere thank to the reviewers for their valuable suggestions and comments. Authors also acknowledge their sincere thank to SERB, New Delhi, Government of India, for providing the financial assistance grant under the research Grant SR/FTP/MS-038/2011.

CONFLICT OF INTEREST

Dr. Ashish Tiwari has received research grant from SERB, New Delhi, Government of India. Mr. Satyendra Singh Chauhan is getting fellowship from SERB, New Delhi, under the above research grant.

HUMAN PARTICIPANTS OR ANIMALS

This article does not contain any studies with human participants or animals performed by any of the authors.

REFERENCES

[1]Ali, N., A. Zaman, M. Sajid, J. J. Nieto, and A. Torres. Unsteady non-Newtonian blood flow through a tapered overlapping stenosed catheterized vessel. *Math. Biosci.* 269:94–103, 2015.
[2]Aroesty, J., and J. F. Gross. Pulsatile flow in small blood vessels I. Casson theory. *Biorheology* 9:33–42, 1972.
[3]Aroesty, J., and J. F. Gross. The mathematics of pulsatile flow in small blood vessels I. Casson theory. *Microvasc. Res.* 4:1–12, 1972.
[4]Bali, R., and U. Awasthi. Effect of a magnetic field on the resistance to blood flow through stenotic artery. *Appl. Math. Comput.* 188:1635–1641, 2007.
[5]Bugliarello, G., and J. Sevilla. Velocity distribution and other characteristics of steady and pulsatile blood flow in fine glass tube. *Biorheology* 7):85–107, 1970.
[6]Chakravarty, S., A. Datta, and P. K. Mandal. Effect of body acceleration on unsteady flow of blood past a time-dependent arterial stenosis. *Math. Comput. Model.* 24:57–74, 1996.
[7]Chaturani, P., and P. N. Kaloni. Two layered poiseuille flow model for blood flow through arteries of small diameter and arterioles. *Biorheology* 13:243–250, 1976.

[8]Chaturani, P., and R. Ponnalagar Samy. A study of non-Newtonian aspects of blood flow through stenosed arteries and its applications in arterial diseases. *Biorheology* 22:521–531, 1985.
[9]Chaturani, P., and R. Ponnalagar Samy. Pulsatile flow of a Casson fluid through stenosed arteries with application to blood flow. *Biorheology* 23:499–511, 1986.
[10]Dash, R. K., G. Jayaraman, and K. N. Mehta. Estimation of increased flow resistance in a narrow catheterized artery—a theoratical model. *J. Biomech.* 29:917–930, 1996.
[11]Elnaqeeb, T., Kh. S. Mekheimer, and F. Alghamdi. Cu-blood flow model through a catheterized mild stenotic artery with a thrombosis. *Math. Biosci.* 282:135–146, 2016.
[12]Lih, M. M. Transport Phenomena in Medicine and Biology, 1st ed. New York: Wiley, 1975.
[13]MacDonald, D. A. On the steady flow through modelled vascular stenoses. *J. Biomech.* 12:13–20, 1979.
[14]Mekheimer, Kh. S., and Y. Abd Elmaboud. Simultaneous effects of variable viscosity and thermal conductivity on peristaltic flow in a vertical asymmetric channel. *Can. J. Phys.* 92:1541–1555, 2014.
[15]Mekheimer, Kh. S., and M. A. El Kot. Mathematical modelling of axial flow between two eccentric cylinders: application on the injection of eccentric catheter through stenotic arteries. *Int. J. Non-Linear Mech.* 47:927–937, 2012.
[16]Mekheimer, Kh. S., and M. A. El Kot. Mathematical modelling of unsteady flow of a Sisko fluid through an anisotropically tapered elastic arteries with time-variant overlapping Stenosis. *Appl. Math. Model.* 36:5393–5407, 2012.
[17]Mekheimer, Kh. S., and M. A. El Kot. Suspension model for blood flow through catheterized curved artery with time-variant overlapping stenosis. *Int. J. Eng. Sci. Technol.* 18:452–462, 2015.
[18]Mekheimer, Kh. S., F. Salma, and M. A. El Kot. The Unsteady flow of a Carreau fluid through inclined catheterized arteries have a balloon (angioplasty) with time-variant overlapping stenosis. *Walailak J. Sci. Technol. (WJST)* 12:863–883, 2015.
[19]Misra, J. C., S. D. Adhikary, and G. C. Shit. Mathematical analysis of blood flow through an arterial segment with time-dependent stenosis. *Math. Model. Anal.* 13:401–412, 2008.
[20]Misra, J. C., and S. K. Ghosh. Flow of Casson fluid in a narrow tube with a side branch. *Int. J. Eng. Sci.* 38:2045–2077, 2000.
[21]Nagarani, P., and G. Sarojamma. Effect of body acceleration on pulsatile flow of Casson fluid through a mild stenosed artery. *Korea Aust. Rheol. J.* 20:189–196, 2008.
[22]Nayfeh, A. H. Introduction to Perturbation Techniques, 1st ed. New York: Wiley, 1993.
[23]Ponalagusamy, R., and R. Tamil Selvi. A study on two-layered model (Casson–Newtonian) for blood flow through an arterial stenosis: axially variable slip velocity at the wall. *J. Frankl. Inst.* 348:2308–2321, 2011.
[24]Ponalagusamy, R., and R. Tamil Selvi. Blood flow in stenosed arteries with radially variable viscosity, peripheral plasma layer thickness and magnetic field. *Meccanica* 48:2427–2438, 2013.
[25]Pontrelli, G. Nonlinear problems in arterial flows. *Nonlinear Anal.* 47:4905-4915, 2001.
[26]Rohlf, K., and G. Tenti. The role of the Womersley number in pulsatile blood flow a theoretical study of the Casson model. *J. Biomech.* 34:141–148, 2001.
[27]Sankar, D. S. Two-fluid nonlinear mathematical model for pulsatile blood flow through stenosed arteries. *Bull. Malays. Math. Sci. Soc.* 35:487–498, 2012.
[28]Sankar, D. S., and K. Hemalatha. Pulsatile flow of Herschel–Bulkley fluid through stenosed arteries—a mathematical model. Int. J. Non-Linear Mech. 41:979–990, 2006.
[29]Sankar, D. S., and K. Hemalatha. A non-Newtonian fluid flow model for blood flow through a catheterized artery—steady flow. *Appl. Math. Model.* 31:1847–1864, 2007.
[30]Sankar, D. S., and A. I. M. Ismail. Two-fluid mathematical models for blood flow in stenosed arteries: a comparative study. *Bound. Value Probl.* 2009:1–15, 2009. https://doi.org/10.1155/2009/568657.
[31]Sankar, D. S., and U. Lee. Two-phase non-linear model for the flow through stenosed blood vessels. *J. Mech. Sci. Technol.* 21:678–689, 2007.
[32]Sankar, D. S., and U. Lee. Mathematical modeling of pulsatile flow of non-Newtonian fluid in stenosed arteries. *Commun. Nonlinear Sci. Numer. Simul.* 14:2971–2981, 2009.
[33]Sankar, D. S., and U. Lee. Two-fluid Casson model for pulsatile blood flow through stenosed arteries: A theoratical model. *Commun. Nonlinear Sci. Numer. Simul.* 15:2086–2097, 2010.
[34]Sankar, D. S., and U. Lee. FDM analysis for MHD flow of a non-Newtonian fluid for blood flow in stenosed arteries. *J. Mech. Sci. Technol.* 25:2573–2581, 2011.
[35]Shit, G. C., M. Roy, and A. Sinha. Mathematical modelling of blood flow through a tapered overlapping stenosed artery with variable viscosity. *Appl. Bionics Biomech.* 11:185–195, 2014.
[36]Shukla, J. B., R. S. Parihar, and S. P. Gupta. Effects of peripheral layer viscosity on blood flow through the artery with mild stenosis. *Bull. Math. Biol.* 42:797–805, 1980.
[37]Shukla, J. B., R. S. Parihar, and B. R. P. Rao. Effects of stenosis on non-Newtonian flow of the blood in an artery. *Bull. Math. Biol.* 42:283–294, 1980.
[38]Siddiqui S. U., N. K. Verma, S. Mishra, and R. S. Gupta. Mathematical modeling of pulsatile flow of Cassons fluid in arterial stenosis. *Appl. Math. Comput.* 210:1–10, 2009.
[39]Sinha, A., G. C. Shit, and P. K. Kundu. Slip effects on pulsatile flow of blood through a stenosed arterial segment under periodic body acceleration. *ISRN Biomed. Eng.* 2013:1–10, 2013. https://doi.org/10.1155/2013/925876.
[40]Srivastava, V. P., M. Saxena. Two-layered model of Casson fluid flow through stenotic blood vessels: applications to the cardiovascular system. *J. Biomech.* 27:921–928, 1994.
[41]Womersley, J. R. Method for the calculation of velocity, rate of flow and viscous drag in arteries when the pressure gradient is known. *J. Physiol.* 127:553–563, 1955.
[42]Young, D. F. Effects of a time-dependent stenosis on flow through a tube. *J. Eng. Ind.* 90:248–254, 1968.
[43]Young, D. F. Fluid mechanics of arterial stenosis. *J. Biomech. Eng.* 101:157–175, 1979.